EVOLUTIONARY BIOLOGY

The timetable of evolution

Andrew H. Knoll[1]* and Martin A. Nowak[2]

The integration of fossils, phylogeny, and geochronology has resulted in an increasingly well-resolved timetable of evolution. Life appears to have taken root before the earliest known minimally metamorphosed sedimentary rocks were deposited, but for a billion years or more, evolution played out beneath an essentially anoxic atmosphere. Oxygen concentrations in the atmosphere and surface oceans first rose in the Great Oxygenation Event (GOE) 2.4 billion years ago, and a second increase beginning in the later Neoproterozoic Era [Neoproterozoic Oxygenation Event (NOE)] established the redox profile of modern oceans. The GOE facilitated the emergence of eukaryotes, whereas the NOE is associated with large and complex multicellular organisms. Thus, the GOE and NOE are fundamental pacemakers for evolution. On the time scale of Earth's entire 4 billion–year history, the evolutionary dynamics of the planet's biosphere appears to be fast, and the pace of evolution is largely determined by physical changes of the planet. However, in Phanerozoic ecosystems, interactions between new functions enabled by the accumulation of characters in a complex regulatory environment and changing biological components of effective environments appear to have an important influence on the timing of evolutionary innovations. On the much shorter time scale of transient environmental perturbations, such as those associated with mass extinctions, rates of genetic accommodation may have been limiting for life.

INTRODUCTION

Deep time and its codification in the geologic time scale stand as the intellectual triumph of 19th century geology (1). Initially, time was marked by the comings and goings of fossils, a relative time scale recognized, after Darwin, as the historical record of evolution. However, with the discovery of radioactivity, the prospect of calibrating geologic time in years arose. In 1907, Arthur Holmes used Bertram Boltwood's research on the radioactive decay of uranium to date ancient terrains in Sri Lanka at 1640 million years, and soon thereafter, Joly and Rutherford argued from pleochroic halos in granite that Devonian rocks are at least 400 million years old (Ma) (2). Despite this, routine application of radiometric dating to Earth history accelerated only half a century later, in conjunction with better instruments and careful mapping of Earth's oldest rocks (3). The calibration of evolutionary history requires that paleobiological and biogeochemical evidence be integrated with accurate and precise geochronology within a spatial framework provided by careful mapping and measured stratigraphic sections. The result is not only a timetable of evolution but also an improved sense of evolutionary rates as they have varied through time. Here, we review applications of increasingly sophisticated geochronological methods that have altered our sense of evolutionary pattern, including both radiations and extinctions. We can identify evolutionary events as fast or slow, but relative to what? Can evolutionary theory provide predictions that can be tested against the empirical record? Is the pace of evolution inferred from geologic history governed largely by genetics, or does environmental change beat the evolutionary tattoo? With these questions in mind, we compare theoretical approaches to evolutionary time scale with the record reconstructed from sedimentary rocks.

CONSTRAINING THE TIMING OF MAJOR EVOLUTIONARY EVENTS
Radiations through Earth history

To begin at the beginning, we can ask when life first gained a persistent toehold on Earth. Following the discovery of microbial fossils much

older than the oldest known animals (4), paleontological and biogeochemical attention turned quickly to Earth's oldest little metamorphosed sedimentary rocks. Radiometric dates soon established that the thick sedimentary-volcanic succession of the Swaziland Supergroup, South Africa, was older than 3 billion years (5), but geologic relationships between dated granites and biologically informative sedimentary rocks remained uncertain and analytical uncertainties were large (6). The Warrawoona Group, Western Australia, was soon shown to be comparably old (7), and with the development of the sensitive high-resolution ion microprobe (SHRIMP), capable of dating single zircons with low analytical uncertainty (8), a highly resolved geochronological framework for the Warrawoona succession was established (9, 10).

Stromatolites, widely accepted as reflecting a microbial influence on accretion, have been documented from the Strelley Pool Formation of the Warrawoona Group (11–13), their age constrained by underlying 3458 ± 1.9–Ma volcanics of the Panorama Formation and the overlying 3350- to 3335-Ma Euro Basalt (9, 14). Putative microfossils have also been reported from the Strelley Pool cherts, as well as from cherts of the 3481 ± 3.6–Ma Dresser Formation (15–17); however, their interpretation remains controversial because simple biological remains can be difficult to distinguish from textures imparted during later hydrothermal alteration (18–20). More compelling, widespread and consistent ^{13}C depletion in organic matter from these and younger Warrawoona units is parsimoniously interpreted in terms of photoautotrophy (21). Evidence from sulfur isotopes is more challenging to interpret, but several lines of evidence also favor the presence of a microbial sulfur cycle at this time (22). Swaziland sedimentary rocks contain a broadly comparable geobiological record, set within a similarly well-resolved temporal framework (23).

Life, then, appears to have been present when the oldest well-preserved sedimentary rocks were deposited (Fig. 1). How much earlier life might have evolved remains conjectural. Reduced carbon (graphite) in ancient metaturbidites from southwestern Greenland has a C-isotopic composition, consistent with autotrophy (24), and recently, upwardly convex, laminated structures interpreted (not without controversy) as microbialites have been reported as well (25); the age of these rocks is constrained by cross-cutting intrusions that cluster tightly around 3710 Ma (25). A

[1]Department of Organismic and Evolutionary Biology, Harvard University, Cambridge, MA 02138, USA. [2]Program for Evolutionary Dynamics, Department of Organismic and Evolutionary Biology, Department of Mathematics, Harvard University, Cambridge, MA 02138, USA.
*Corresponding author. Email: aknoll@oeb.harvard.edu

still earlier origin for biological carbon fixation is suggested by a ^{13}C-depleted organic inclusion in a zircon dated at 4100 ± 10 Ma (26), although it is hard to rule out abiological fractionation in this minute sample of Earth's early interior.

A second milestone in the history of life was the initial rise of oxygen in the atmosphere and surface oceans, an event known as the Great Oxygenation Event (GOE) (Figs. 1 and 2) (27). An environmental transition of key biological importance, the GOE is recorded geologically and geochemically, most notably (and quantitatively) by the end of large mass-independent sulfur isotope fractionation in sedimentary sulfides and by the last appearances of redox-sensitive minerals as detrital grains in sedimentary rocks. South African rocks that record the S-isotopic shift lie above volcanic beds dated by SHRIMP U-Pb zircon geochronology at 2480 ± 6 Ma and below pyritiferous shales dated by Re-Os methods at 2316 ± 7 Ma (28). The last appearance of redox-sensitive detrital minerals is constrained to be younger than 2415 ± 6 Ma by a SHRIMP U-Pb date for zircons in an underlying ash bed (29), whereas recent analysis of an overlying volcanic unit yields a date of 2426 ± 1 Ma
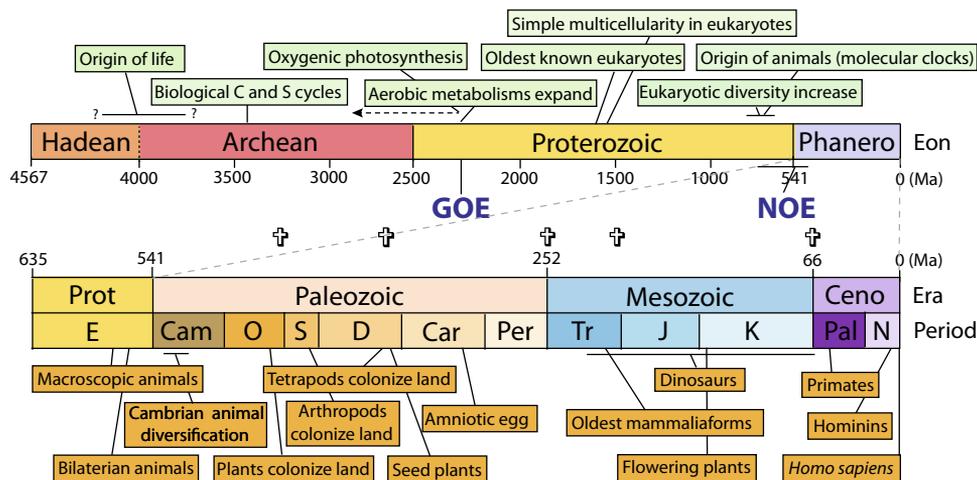
Fig. 1. The evolutionary timetable, showing the course of evolution as inferred from fossils, environmental proxies, and high-resolution geochronology. Phanero, Phanerozoic; Prot, Proterozoic; Ceno, Cenozoic; E, Ediacaran; Cam, Cambrian; O, Ordovician; S, Silurian; D, Devonian; Car, Carboniferous; Per, Permian; Tr, Triassic; J, Jurassic; K, Cretaceous; Pal, Paleogene; Neo, Neogene. Crosses indicate times of major mass extinctions.
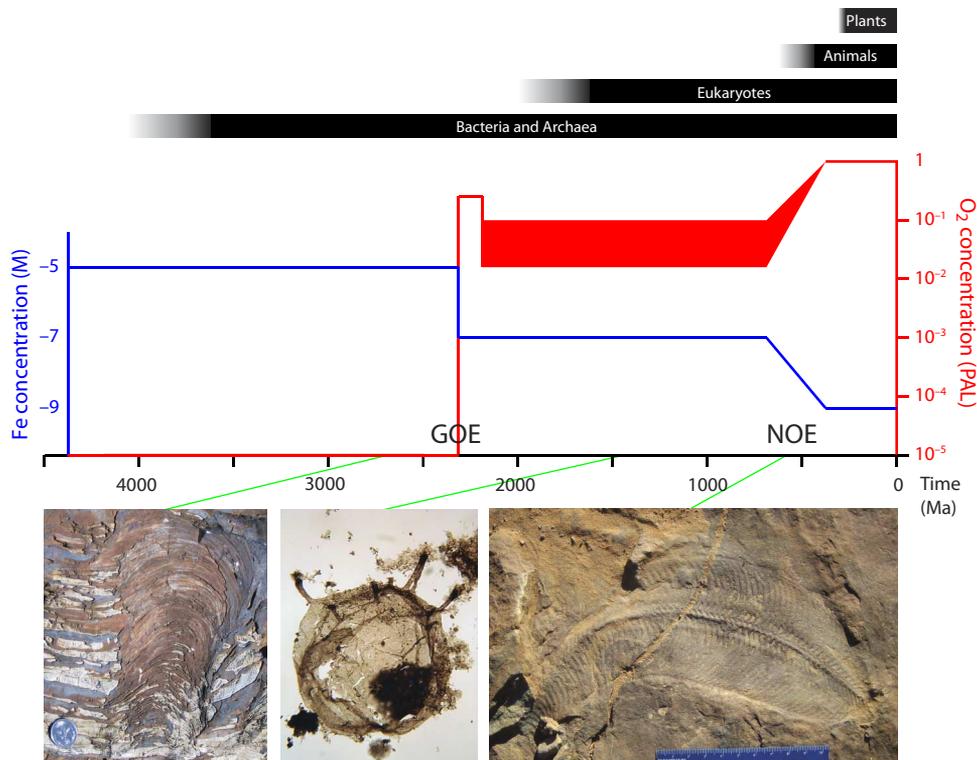
Fig. 2. The geologic history of Fe in seawater and O$_2$ in the atmosphere and surface ocean. Fossil images from left to right show biogenic stromatolites, accreted by microbial mat communities (2700 Ma; Fortescue Group, Australia), an early eukaryotic microorganism (1400 to 1500 Ma; Roper Group, Australia), and an Ediacaran metazoan (543 Ma; Nama Group, Namibia). PAL, present atmospheric level.

(30). Thus, geochronology and geochemistry together place sharp constraints on the timing of the GOE and, therefore, the minimum age of oxygenic photosynthesis and the diversification of oxygen-requiring metabolic and biosynthetic pathways (31).

Moving forward in time, the record grows richer, calibrated by high-resolution U-Pb analyses of zircons from ash beds interbedded with biologically informative rocks and, increasingly, Re-Os analyses of carbonaceous shales that actually contain key paleobiological records. Eukaryotic cells evolved phagocytosis, increasing the role of predation in microbial ecosystems; protists also established a genetic and cell biological foundation for the later evolution of complex multicellularity. The oldest microfossils of probable eukaryotic affinities are large (>100 μm), faintly ornamented vesicles from the Changzhougou Formation, China (32). Conventionally described as 1800 to 1600 Ma, Changzhougou fossils are now constrained to be younger than the 1673 ± 10–Ma U-Pb age of zircons in a granite-porphyry dike that cuts underlying rocks and older than the 1625.3 ± 6.2–Ma ash bed in overlying beds (33). Shales (1600 to 1400 Ma) distributed globally contain similar assemblages of moderately diverse microbial eukaryotes [reviewed by Javaux and Knoll (34)] as well as simple multicellular forms (35, 36), but the oldest fossil population reliably assigned to a crown group eukaryotic taxon comprises simple multicellular red algae preserved in silicified carbonates from Arctic Canada only loosely constrained to be ca. 1200 to 1100 Ma (37).

The eukaryotic fossil record expands to include vase-shaped protistan tests (38), mineralized scales (39), and an increasing number of ornamented cell walls and coenocytic taxa (40, 41) in rocks deposited during or after the Bitter Spring carbon-isotope anomaly, constrained by an 811.51 ± 0.25–Ma ash bed just below its onset (42). Increasing time resolution in Neoproterozoic paleontology is exemplified by taxonomically similar multispecies protist assemblages formed 4000 km apart but of indistinguishable age, within the resolution of radiometric dating (43). Molecular clocks suggest that animals were part of the mid-Neoproterozoic diversification of eukaryotes (44), although animal body fossils occur only in younger rocks. In addition, later Neoproterozoic rocks record renewed redox transition, sometimes christened the Neoproterozoic Oxygenation Event (NOE) (Figs. 1 and 2) (45). Some evidence, for example, from selenium isotopes (46), suggests that the NOE began as early as 750 Ma, whereas diverse geochemical data indicate Ediacaran acceleration (47) and still other proxies (Fe speciation and Mo isotopes) suggest that the permanent oxygenation of deep oceans occurred only within the Paleozoic Era (48, 49). The precise nature and timing of this transition remains a subject of research, reflecting incomplete and sometimes contradictory geochemical results, limited radiometric calibration, insufficiently appreciated diagenetic influences, and, very possibly, a complex temporal pattern of oxygen fluctuation before a new steady state was achieved (50). What is clear is that the NOE encompasses the initial radiation of large, complex animals. The diversification of animals occurred within the context of the NOE, likely reflecting both new physiological opportunities attendant on increasing PO_2 (partial pressure of oxygen gas) (51) and, possibly, feedbacks from emerging animals onto marine redox profiles (52).

From our current perspective, it might seem surprising that 25 years ago, there was no consensus on the age of the Proterozoic-Cambrian boundary or of rocks on either side of the boundary that preserve fossils of early animals. The fact that we have an increasingly refined temporal framework for early animal diversification today owes much to the work of Samuel Bowring (Fig. 1). Isotope dilution thermal ionization mass spectroscopy (ID-TIMS) provides U-Pb ages of unprecedented accuracy and precision and is especially useful when zircons have experienced a complex geological history (53). Modern attempts to construct a timetable of early animal evolution began with ID-TIMS dating of zircons from a volcanic breccia intercalated among Siberian siltstones that contain basal Cambrian skeletal fossils (54). The published date of 543.9 ± 0.25 Ma has since been complemented and refined by U-Pb dates from ash beds in Namibia, Oman, and China, leading to a consensus age of 541 ± 1 Ma for the Proterozoic-Cambrian boundary (55–57). Fossils record the sequential evolution of bilaterian body plans and diversity during the first half of the Cambrian Period, with much of the action taking place after 525 Ma (58, 59); however, the soft-bodied fossils that illuminate Cambrian evolution with exceptional brightness are only moderately well placed in time. Because none of these are directly constrained by radiometric dates, their ages are estimated on the basis of biostratigraphic correlation with successions that contain dated volcanic rocks. On this basis, the Sirius Passet fauna in Greenland (60) is considered to be about 520 Ma; the remarkably diverse Chengjiang fauna (61) in China is perhaps a few million years younger, and the Emu Bay fauna in Australia (62) is a bit younger than that. All are older than 514.45 ± 0.36 Ma (63). The Burgess Shale, most famous of all exceptionally preserved Cambrian faunas, is constrained to be younger than 510 ± 1 Ma and older than 503.14 ± 0.13 Ma (59). Collectively, then, fossils tell us that diverse animal body plans emerged during the first 30 million years of the Cambrian Period, with stem group members of extant phyla and classes dominating marine faunas (64).

Looking backward from the Proterozoic-Cambrian boundary, the oldest known animal body fossils, osmotrophic metazoans, ascribed to early branching, occur in rocks constrained from below by a 570.94 ± 0.38–Ma ash bed and from above by another ash, dated at 566 ± 0.35 Ma (65), with greater body plan diversity emerging only later. Trace fossils interpreted in terms of bilaterian locomotion also occur in ca. 565-Ma basinal strata from Newfoundland (66), whereas additional bilaterian trace fossils, body fossils, and microscopic cuticle remains occur in successions on the East European Platform younger than 558 ± 1 Ma (67–69); simple skeletonized metazoans occur only in rocks deposited during the last 8 to 9 million years of the Ediacaran Period, constrained by a U-Pb zircon date of 547.32 ± 0.66 Ma for an ash bed within the lowermost skeleton-bearing carbonates (55, 56, 70).

During the Paleozoic Era, evolutionary innovation moved onto land, as plants and, subsequently, at least nine clades of animals established what would become Earth's most diverse, productive, and biomass-rich ecosystems. Age estimation becomes increasingly refined as we move upward in time, with more abundant fossiliferous successions and more highly resolved biostratigraphic zonation. Increasingly, the calibration of evolutionary events is based not on the direct dating of key fossiliferous horizons but on radiometric constraints placed on successions that can be correlated with key fossil horizons. For example, Husson et al. (71) dated six ash beds in a basal Devonian sedimentary succession, yielding an estimate of 421.3 ± 1.2 Ma for the beginning of the Devonian Period. Similarly, 377.2 ± 1.7–Ma ash beds just below the Upper Kellwasser Horizon in Germany constrain a widely correlated biogeochemical event associated with the extinction of reef faunas (72).

These dates provide calibration points for the origin and diversification of land plants and animals (Fig. 1). Spores and cuticle in Middle Ordovician (ca. 470 Ma) deposits document plants with morphological and life cycle complexity broadly similar to those of extant liverworts (73), with possible progenitors in rocks as old as Cambrian Series 3 [ca. 510 to 500 Ma (74)]. True vascular plants evolved no later than the later Silurian Period [ca. 423 Ma (75)], followed by a marked

Devonian radiation of vascular plants with complex organography: Plants began the period as centimeter-scale, naked photosynthetic axes and exited it with leaves, roots, wood, and the seed habit (73). A key deposit that has been dated directly is the Rhynie Chert, Scotland, whose superb anatomical preservation (76) provides paleobotany's equivalent to the Burgess Shale. $^{40}Ar/^{39}Ar$ dates on potassium feldspar associated with the hydrothermal fluids that preserved Rhynie plants yield a mean date of 407.1 ± 2.2 Ma (77).

Chelicerates, including both arachnids and scorpions, occur as fossils as early as ca. 420 Ma (78), as do myriapods (79). Early diverging insects have been recognized in the Rhynie Chert (80). Thus, invertebrate components of terrestrial ecosystems closely followed plants onto land. However, tetrapod vertebrates did not gain the land until well into the Devonian Period, with a succession of fossils showing increasing evidence of terrestrialization from 380 to 365 Ma (81, 82).

The final stop in this whirlwind tour of the evolutionary timetable is ourselves. The ages of hominin (the lineage leading to Homo sapiens, sister to chimps and bonobos) fossils are estimated on the basis of high-resolution geochronology (mostly $^{40}Ar/^{39}Ar$) on ash beds intercalated among fossiliferous sediments, supplemented by a well-calibrated magnetic stratigraphy. Although rare, early hominins have been found in several localities in Africa, with ages of around 6 million years, and a recent discovery suggests human-gorilla divergence as early as 8 Ma (83). In turn, the oldest fossil attributed to the genus Homo is a mandible with teeth, found in siltstone 10 m above a 2.822 ± 0.006–Ma ash bed but older than a superjacent tuff dated at 2.669 ± 0.011 Ma (84); the fossil in question combines features characteristic of Homo and Australopithecus, raising the question of how we should define our own genus (85). In Kenya and Ethiopia, possible Homo erectus bones have been discovered just below an ash bed dated at 1.87 ± 0.02 Ma (86, 87), and both a more securely identified H. erectus cranium and Acheulian stone tools (generally associated with H. erectus in Africa) occur just above a 1.74 ± 0.06–Ma ash bed (88). H. erectus remains in Asia independently indicate an origin of more than 1.7 Ma (89, 90). Anatomically modern humans (Homo sapiens sapiens) emerged after 200,000 years ago [constrained by $^{40}Ar/^{39}Ar$ ages of 196 ± 2 thousand years on volcanic ash within a fossiliferous unit (91)], dispersing to the Levant by 100,000 years ago and, later, around the world. Uncertainty in dates for human dispersal reflects both the limited availability of fossils and differing opinions about what constitutes a modern human [summarized by Grove (92)], but recent molecular clock analyses suggest that the ancestors of modern Eurasian populations migrated from Africa 50,000 to 70,000 years ago, with Papuan genomes suggesting a small admixture of genes from a population that migrated earlier but is now extinct (93–95). From there, it is but a geologically short hop to agriculture (ca. 11,500 years ago) and onward to the Industrial Age technologies and exponential population growth that has established our species' unprecedented ecological footprint on Earth system.

Clearly, the integration of geochronology and paleontology in carefully measured stratigraphic sections has done much to resolve the timetable of evolution. In addition to new fossils and improved analytical techniques, continued improvements in time resolution will benefit from expanded radiometric calibration of chemostratigraphic variations and paleomagnetic reversals in sedimentary successions—critical when fossils are scarce, as in the Proterozoic record (42); expanded application of astrochronometry, exploiting orbitally driven periodic variations in accumulating strata (96); and the development of improved Bayesian models for projecting time and uncertainties between dated horizons within a succession (97).

The timing and rapidity of mass extinctions

The fact that diversity declined and faunas changed markedly at discrete times in Earth history was well known to 19th century scientists (98); the most prominent of these changes—now understood to reflect mass extinctions—dictated the subdivision of Phanerozoic time into the Paleozoic, Mesozoic, and Cenozoic eras. Despite this, mass extinction figured only peripherally in discussions of evolutionary history until 1980, when Alvarez et al. (99) hypothesized that bolide impact at the end of the Cretaceous Period devastated the planet, eliminating nonavian dinosaurs and many other taxa. The Alvarez paper was a hypothesis about mechanism but also about timing and rate. Chemical, mineralogical, and sedimentological features attributable to impact were identified in extinction-level strata, and subsequently, a massive crater was recognized beneath the current surface of the Yucatan Peninsula (100). Critically, $^{40}Ar/^{39}Ar$ dates on Haitian tektites generated by the Chicxulub impact are essentially indistinguishable from those on a bentonite 80 cm above the mass extinction horizon in Montana: 66.038 ± 0.25 Ma versus 0.66.019 ± 0.021 Ma, respectively (101). Thus, geochronology provides key support for the Alvarez hypothesis, and conversely, it is accurate and precise geochronology that keeps Deccan Trap volcanism in the discussion of biologically important geophysical changes near the Cretaceous-Paleogene boundary (102, 103).

Phanerozoic rocks record five episodes of major diversity decline, along with a dozen or more smaller extinction episodes (104). Early optimism that impact might provide a general mechanism for mass extinction faded; however, to date, only end-Cretaceous extinction is securely tied to bolide impact. In contrast, massive volcanism has emerged as the leading candidate for at least two major extinctions. Notably, Siberian Trap volcanism is widely accepted as the trigger for the largest known extinction event, at the end of the Permian Period. U-Pb zircon dates for ash beds in China that bracket the extinction constrain its timing to between 251.941 ± 0.037 Ma and 251.880 ± 0.031 Ma (105), indistinguishable from a 251.901 ± 0.061–Ma U-Pb date for the major phase of Siberian Trap eruption (106). Thus, geochronology establishes the synchroneity of volcanism and extinction, but it also does more, emphasizing the rapidity of the extinction and the events that surrounded it (107). In principle, massive volcanism could drive extinction via volatile release, leading to global warming, ocean acidification, and oxygen depletion in subsurface ocean waters. However, for these mechanisms to work, the time scale of emission must be fast (108, 109). The Siberian traps pass this test, thereby providing both a trigger and physiological kill mechanisms for end-Permian extinction.

Increasing evidence now links end-Triassic mass extinction with massive volcanism as well (110), and at least some minor extinctions during the Mesozoic Era also coincide with massive volcanism (111). An unanswered question relevant to our environmental future is why some massive volcanic events caused mass extinction, whereas others did not. In any event, the conclusion that CO_2 is currently increasing at rates not seen during the preceding 66 million years (112) should give us pause.

Evolutionary rates inferred from a time-calibrated fossil record

Paleontological inference of evolutionary rate is rooted in Simpson's (113, 114) influential contributions to the neo-Darwinian synthesis. Simpson recognized that fossils document changes in morphology and diversity through time, making it possible to estimate rates of evolution over long time intervals. He also understood that, in principle, fossils might enable biologists to gauge rates of genetic change through

time, although he lamented that the basis for doing this was not then available. Like the evolutionary timeline itself, geologic inferences of evolutionary rate depend on a well-documented fossil record, high-resolution geochronology to establish a timeframe, and, increasingly, well-resolved phylogenies (115). When these are in place, geologic data can provide calibration points for estimating rates of speciation and extinction, morphological change through time, and molecular sequence change within and among lineages.

Fossil taxa with numerous occurrences within a time-calibrated stratigraphic interval permit one to estimate rates of morphological change within lineages, providing critical insights into these influential and controversial hypotheses as punctuated equilibrium and the biological processes that govern phenotypic change through time (116). Analysis of several hundred examples indicates that on time scales of 5000 to 50,000,000 years, patterns of sustained directional change are seldom observed in fossil sequences (116, 117). Consequently, net rates of morphological change within lineages are commonly low, a pattern that led Stanley (118) to suggest that infrequent spurts of morphological change must account for larger-scale paleontological pattern. The fact that directional change is rarely sustained over long time intervals helps in explaining the inverse relationship between the rate of morphological evolution and the time scale over which it is measured, originally argued by Gingerich (119, 120). Although dismissed early on as an artifact of plotting t versus $1/t$ (121), the relatively high rates of morphological change observed in some microevolutionary experiments and field observations can be reconciled with lower rates of net long-term change if morphological evolution is commonly discontinuous or reverses direction. Raup and Crick (122), for example, concluded that morphologic evolution in the Jurassic ammonite *Kosmoceras* "was governed in large part by directional selection with fairly frequent changes in the direction of selection." Sediment accumulation—the archive of the fossil record—itself shows a pattern of decreasing rate with longer time scales of observation, indicating that sediment deposition is both episodic and prone to offset by erosion (123).

Scaling upward, time-calibrated fossil sequences can also document patterns of morphological change among lineages within a clade. In his discussion of morphological rates, Simpson highlighted Westoll's (124) classic analysis of lungfish evolution. Westoll scored morphological character states for fossil and living lungfish and plotted them as a "modernization" index through time; the results suggest rapid character evolution early in the history of the clade, with relatively little subsequent change. Lloyd (125) revisited lungfish evolution more recently, now in the context of better fossils, an improved timeframe, and an explicit phylogenetic hypothesis; his analysis shows pulses of relatively strong character change after the initial radiation of the group but broadly corroborates the pattern of decreasing rate of character innovation identified by Westoll. However, such a pattern is not necessarily generalizable. For example, in a discrete character-based analysis of echinoid echinoderms, initial rates of morphological evolution were slow, later peaking episodically in association with functional innovations (126). Taxonomic restriction to irregular echinoids yields a more Westollian pattern of rapid change early in clade history, highlighting the importance of phylogenetic and temporal scale in morphologic analyses (126).

Morphospace analyses, in which taxa are plotted within a multidimensional space whose axes are morphological variables, provide another perspective on clade-level morphological change through time. For groups that range from Cambrian arthropods (127) and Paleozoic crinoids (128) to early vascular plants (129) and diatoms (130), many clades show rapid morphological diversification early in their history,

followed by species diversification within the morphological boundaries established earlier (131). In evolution, then, disparity commonly precedes diversity. Recently, morphospace analyses have incorporated phylogenetic information [documenting morphological trajectories within and between clades (132)], but to date, few studies have made explicit or quantitative use of geochronological constraints.

Geochronology plays a larger role in studies of taxonomic rate: that is, rates of speciation and extinction through time. Once again, early attempts to compare taxonomic rates can be found in Simpson's writings; for example, he argued that mammals have shorter species durations—and, therefore, higher extinction rates—than marine bivalves [see also the study of Stanley (118)]. One need only look at phylogenies to recognize that rates of diversification can markedly differ between closely related taxa (133, 134). Paleontological analyses of taxonomic rate have expanded in parallel with comparative biological studies, gaining particular traction with the advent of paleontological databases, most notably through the pioneering research of Sepkoski (135). Sepkoski (136) estimated per-taxon rates of origination for genera in a wide variety of marine animal classes, finding that groups that were most prominent in the Cambrian had significantly higher rates of origination (and extinction) than those that dominate later marine diversity. Within-taxon analyses also provide evidence of declining turnover rates through time. For example, Foote (137) estimated that the median generic longevity for Cambrian trilobites was about 2.1 million years, compared with 6.3 million years for Ordovician genera; subsequent calibration of the Cambro-Ordovician time by U-Pb geochronology amplifies the differences between periods, indicating that, on average, Cambrian trilobite genera lasted only about a million years (54). Cambrian trilobites show greater morphological variability within species than younger members of the group (138). More generally, Gilinsky and Bambach (139) argued for both declining rates of origination and increasing rates of extinction through the Phanerozoic Eon, which, along with observations of increased speciation rates in the aftermath of mass extinctions, suggests diversity dependence in taxonomic rates and, therefore, ecological limits to diversity change through time (140). Consistent with this, Bush *et al.* (141) have shown that Cretaceous-Cenozoic increase in taxonomic richness among marine animals has been driven almost exclusively by diversification among animals that copulate or otherwise directly deliver sperm to females; animals that broadcast eggs and sperm have not diversified over this interval, implicating life cycle dynamics in diversity-dependent evolution. A comparable argument has been made for vascular plants, where faithful animal pollination may similarly have freed plants from limits on population density and, therefore, community diversity imposed by wind pollination (142). However, additionally, because of changing physical and biological conditions, environmental carrying capacities have almost undoubtedly varied through time, complicating ecologically inspired interpretations of taxonomic rates (143, 144).

Macromolecular sequence data permit one to estimate rates of molecular evolution, provided that the data can be arrayed within a well-supported phylogeny and at least some fossils of known phylogenetic position can be dated by accurate and precise geochronological methods. Early assumptions of rate invariance among clades have been replaced by algorithms that recognize and incorporate observed patterns of rate variation, permitting new insights into patterns of molecular evolution through time. The relevant literature is large and growing, underpinning molecular clock estimates for groups as varied as cyanobacteria (145), eukaryotes (146, 147), metazoans (44), land plants (148), mammals (149), and more. Here, we note only that improved radiometric

constraints play an important, if underappreciated, role in ongoing studies of molecular rates and clocks. When sequence data are assembled for groups with an excellent fossil record, strong time constraints, and a well-supported phylogeny, these data can be used to test different hypotheses for the biological drivers of genetic evolution [for example, see the study of Ezard *et al.* (*150*)]. As is the case for phenotypic rates, rates of molecular change vary widely within and among clades, although the relationship between phenotypic and genotypic rates is unclear.

At the broadest level, fossils may suggest an acceleration of evolution through time. Proterozoic protists, for example, turned over more slowly than their Phanerozoic counterparts, perhaps reflecting evolution in ecosystems with or without animals (*151*, *152*). However, support for accelerating rates is less obvious if we consider metabolic, histological, or molecular evolution. The evolvable morphologies of animals and plants have enabled continuing functional and behavioral innovations through Phanerozoic time, along with increasing diversity on land and in the oceans. This stands in apparent contradistinction to the long antecedent interval of Proterozoic time commonly caricatured as the "boring billion," but it was this earlier interval, when features of eukaryotic cell biology and genetic regulation evolved, that made animal evolution possible. Of the eight major transitions in evolution proposed by Maynard Smith and Szathmáry [see review by (*153*)], only eusociality and language postdate the Proterozoic Eon—given that this list does not include metabolic innovations such as photosynthesis and nitrogen fixation, the evolutionary importance of early Earth history is even more pronounced (*154*).

Taken collectively, the immense span of biological history, the varying perceptions of key evolutionary events, the existence of mass extinctions, and substantial variations through time and among taxa in both molecular and phenotypic rates of change prompt the question of whether there is such a thing as an intrinsic rate of evolutionary discovery. Do rates of genetic change govern the rates of phenotypic change documented in the geologic record, or are observed rates of change conditioned by environmental dynamics and the biological context of evolving lineages? To consider this further, we must look to evolutionary theory.

A THEORETICAL FRAMEWORK FOR THE EVOLUTIONARY TIMETABLE

Evolutionary theory can make statements about the time scales associated with evolutionary dynamics. The results that are best understood concern the rates at which individual mutations occur and reach fixation or become extinct. For example, we can estimate the time scale on which populations of viruses, bacteria, or cancer cells accumulate point mutations that confer resistance to treatment (*155*, *156*), or we can estimate the times until microbial populations discover adaptations based on individual point mutations or other small genetic alterations (*157*–*161*). But what can we say about the longer evolutionary time scales that are relevant for the events reviewed here? How long would it take for a planet of bacteria to discover the tools required for oxygenic photosynthesis or a world of prokaryotes to construct eukaryotes by endosymbiosis?

Today, an estimated 10^{30} bacteria populate Earth. Most of these cells live in the ocean, where they divide, on average, every 1 to 10 days (*162*). If these estimates hold for the past, the billion years recorded by Archean sedimentary rocks should have experienced about 10^{41} cell divisions. On early Earth, population sizes and reproductive rates might well have been different, but even if modern estimates are off by several orders of magnitude, the number of Archean cell divisions must still have been impressive. What can evolution discover with this reproductive potential, and how long would such a process take?

Progress toward answering such a question depends on our understanding of the mechanisms by which evolution discovers new functions. Evolutionary innovations lead to qualitatively new phenotypic traits. They can be caused, for example, by new genes, new combinations of genetic material, new regulatory circuits, and new metabolic networks (*163*–*165*). In the world of complex organisms, evolutionary innovation could be the emergence of a new organ or a new tissue or the expression of a gene in a novel cell type (*166*). Here, we adopt the perspective that the fundamental basis of every evolutionary innovation is a modified genetic sequence. Even phenotypic plasticity is ultimately encoded genetically. In the following, we mostly consider evolutionary innovation in the world of prokaryotes.

Evolution is a search process. The search occurs in the high dimensional space of genetic sequences. The steps in this space include point mutations, insertions, deletions, and genetic rearrangements. Evolutionary innovation can include fusion or amplification of genes, of parts of genes, bringing together distinct genes in a single cell and bringing the expression of a gene under the control of new promoter. Imagine that a new function, not currently present in a bacterial population, requires a new gene of length L. The average bacterial gene is $L = 1000$ nucleotides long, so one possibility to imagine the search for new function is to consider a bacterial population exploring the hypercube of sequence space containing L dimensions and 4^L sequences. Attainment of a new function will depend on the structure of the existing protein encoded by the gene. Because there is redundancy on the level of the genetic sequence, any particular protein structure can be encoded by many different genetic sequences. Therefore, the searching population would not be required to find a unique sequence. In principle, the space of 4^L sequences will contain many solutions, and these solutions might be widely distributed in sequence space. Nevertheless, one can show that the search for solutions of $L = 1000$ can quickly exhaust the evolutionary potential of an entire planet unless the solutions are so abundant that even random sequences might contain them with high probability. The straightforward evolutionary search leads to a strongly dichotomous result: (i) The solution is hyper-abundant so that random sequences can solve the task or (ii) the solution will almost certainly not be found by an entire planet of bacteria searching for a billion years (or more).

How then does evolution discover new functions whose target sequences are not hyper-abundant? One mechanism that can solve the problem is the "regeneration process," in which the genetic machinery of the population regenerates starting sequences by means of gene recombination and/or duplication that are a certain number of steps, say k, away from a target sequence (Fig. 3) (*167*). Those steps can include point mutations, insertions, deletions, and genomic rearrangements. It could be that some steps need to occur in a particular order, whereas others can occur in any order. Therefore, the regeneration process can include epistatic interactions between mutations and potentiating mutations (*167*). We envisage the regeneration process as a sequence of steps that are not individually favored by natural selection. Only the final product is favored by natural selection. If individual steps are already favored, then the evolutionary dynamics would describe the stepwise improvement of an existing function rather than the discovery of a new function. The incremental adaptation would certainly occur quickly on a geological time scale.

Most ensuing searches in the regeneration process will immediately lead away from the target and so fail with high probability. The average time until a single search hits the target would be exponential in L. However, the starting condition is regenerated all the time, with unsuccessful searches being discarded. The result is that we need only
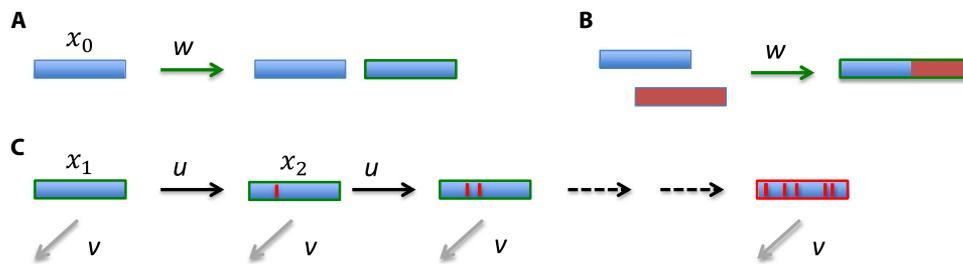
Fig. 3. The regeneration process. Gene duplication (**A**) or recombination (**B**) generates a starting condition for the search process, at rate w. (**C**) From the starting condition, we require k mutational steps, each at rate u, to reach the target sequence, which encodes a new function. At each step, there is the possibility to receive inactivating mutations, at rate v, which destroy the search. The frequency of the wild type is denoted by x_0. The frequencies of the intermediate steps in the search process are denoted by x_i. At steady state and assuming neutrality, we have the following frequencies: $x_0 = \frac{v}{v+w}$ and $x_i = \left(\frac{w}{u}\right)\left(\frac{v}{v+w}\right)\left(\frac{u}{v+u}\right)^i$. Let us consider a numerical example: $w = 10^{-7}$, $u = 10^{-9}$, $v = 10^{-7}$ per cell division. Then, cells that have made as many as 10 steps toward the target have a frequency of about 5×10^{-19} and are present on a planetary scale with a total cell number of the order on 10^{30}.

polynomially many searches in L to find the target with high probability. That is, the search time is exponential in k but not in L. Sexual reproduction and exchange of genetic material can further increase the efficiency of the search processes by a linear factor.

With the regeneration process, a planet of bacteria seems well equipped to discover new functional tools on a time scale that is geologically rapid. Our modeling exercise suggests that as the environment calls for new functions to be advantageous, the relevant sequences might already preexist in the population, either fully or partially formed. The coming together of such sequences in single cells can then lead to genetic machinery able to exploit a new ecological niche.

The GOE and its biological consequences
Armed with the preceding results, we can take a closer look at the timing and dynamics of the GOE. As introduced earlier, the GOE represents the moment in geologic history when O_2 in the atmosphere permanently rose above a threshold of about 10^{-5} of its present-day level (168). There is reason to believe that oxygenation was protracted, with O_2 increasing to levels perhaps comparable to today's over some 200 million years, before declining to the relatively low values thought to characterize most of the Proterozoic Eon (169, 170). A growing number of geochemical analyses also suggest that low levels of oxygen built up at least locally and transiently within the water column or in benthic mat communities as early as 3 billion years ago (171). Thus, available geochemical data indicate that either oxygenic photosynthesis evolved 2.4 billion years ago and rapidly oxygenated the atmosphere and surface oceans (requiring that all geochemical evidence for earlier local oxygenation be interpreted in terms of later oxic diagenesis) or that oxygen consumption matched production for the first several hundred million years of cyanobacterial history. In the latter case, the threshold represented by the GOE would reflect a decreasing supply of oxidants from volcanic gases, hydrothermal fluids, and basaltic rocks; increased rates of oxygenic photosynthesis; increased hydrogen escape from the top of the atmosphere; or some combination of these (171, 172). Total rates of primary production would have been set by nutrient availability, especially P. Because of adsorption onto iron hydroxides and removal by incorporation into vivianite in anoxic environments, P availability is thought to have been low in Archean oceans, and although somewhat higher in Proterozoic seas, it was still well below Phanerozoic values (173–177). In turn, the proportional importance of oxygenic photosynthesis would have reflected Fe/P, with anoxygenic photosynthesis favored as long as electron donors such as ferrous iron were available (176).

Wherever and whenever O_2 first accumulated, life figures prominently in its causation and consequences. Oxygenic photosynthesis is generally accepted as necessary for terrestrial oxygenation (178), requiring coupled photosystems I and II in all their molecular complexity (179). Similarly, early oxygenation made the origin and expansion of aerobic respiration, as well as the diversification of oxygen-requiring biosynthetic pathways, possible (31). Cyanobacteria are ecosystem engineers: Once O_2 began to accumulate in the surface ocean, alternative electron donors were eliminated.

What, then, governed the timetable of the GOE and its biological consequences? Was it influenced most strongly by the time scale on which mutations could result in adaptations for the production and utilization of oxygen? Or does natural selection discover physiological adaptations quickly, shifting focus onto environmental history? Given the geochemical evidence that cyanobacteria, and thus oxygenic photosynthesis, preceded the GOE by as much as several hundred million years, it is unlikely that the exact timing and dynamics of the GOE are explained by the evolution of oxygenic photosynthesis per se. Instead, we can imagine that there was a particular steady state between the concentration of oxygen and the biomass of cyanobacteria before GOE. The steady-state level of oxygen is given by the rate of production from cyanobacteria divided by the rate of oxygen removal.

Let x denote the biomass of cyanobacteria and z the concentration of oxygen in the atmosphere. The time derivative of oxygen concentration $\dot{z}$ can then be stated in terms of a simple equation, $\dot{z} = ax - bz$, where the rate of O_2 production is proportional to the abundance of cyanobacteria, ax, and the O_2 removal rate is proportional to the abundance of oxygen, bz. The parameters a and b are appropriate rate constants. The steady-state level of oxygen, $z = ax/b$, is proportional to the abundance of cyanobacteria. Given this, the GOE could reflect an increase in the abundance of cyanobacteria as they evolved to be better competitors in the global ecosystem. In this case, the ratio z/x would remain constant, and the rate constants a and b would not change. Another possibility, favored by us, is that the physical environment of the planet changed, leading to a decline in the rate constant, b, for oxygen removal. This could be caused, for example, by the growth of stable continental cratons, a decline in volcanic emissions of reduced gases and ions, a change in the flux of hydrogen out of the top of the atmosphere, or some combination of these processes (173). If b declines, then the steady-state level of oxygen increases, but the ratio z/x also increases. The accumulation of O_2 in the atmosphere and surface ocean would sweep alternative electron donors from most parts of the photic zone. Thus, anoxygenic photosynthetic bacteria dependent on Fe^{2+} or H_2S for photosynthesis would become strictly limited—a decline in Fe/P, in the formulation of Jones et al. (176)—permanently favoring primary production by cyanobacteria.

The accompanying box and figure present a deliberately oversimplified model for ecosystem change at the GOE. The main inference we draw from this is that whereas rates of oxygen removal might have declined gradually through time, the transition to an oxic atmosphere and surface ocean, with cyanobacteria dominating photosynthesis, would have occurred rapidly once a critical threshold was reached. Ward et al. (180) modeled the GOE as the initial appearance of oxygenic photosynthesis but similarly concluded that the oxic transition was rapid.

Our simple model of bacterial sequence evolution, introduced above, would suggest that shifting redox conditions would quickly be exploited by bacteria with novel physiologies that make use of oxygen in energy metabolism or biosynthesis. Support for this comes from molecular clock estimates of ca. 2310 Ma for the origin of sterol biosynthesis, an oxygen-requiring pathway (181).

The broader theoretical challenge of Earth's timetable of evolution

The GOE played out in a world populated by Bacteria and Archaea, but what about the NOE and beyond? Renewed oxygenation in the Neoproterozoic Era and the temporally associated rise of eukaryotic phytoplankton to ecological prominence could be amenable to modeling broadly similar to that outlined for the GOE. As noted earlier, the pattern of redox change in Neoproterozoic to Early Paleozoic oceans is debated, with estimates for when PO_2 reached 50% PAL ranging from 800 Ma (182) to the Cambrian Period or later (49). However, in general, full oxygenation of ocean basins appears to have been achieved more than transiently only in the Paleozoic Era (48, 49). Renewed oxygenation could have been driven by supercontinental breakup, increasing organic carbon sequestration in newly formed and rapidly subsiding basins. Increased P supply from the weathering of Neoproterozoic large igneous provinces (183, 184) could also have pushed Earth system to a new redox state, which, in turn, would have reduced iron-based sinks for P (177). Eukaryotic phytoplankton and macroscopic animals with high demand for oxygen diversified in the context of this change. Phytoplankton radiations may reflect increased nutrient supply (185), whereas animal radiation likely reflects the consequent increase in food supply and PO_2 increase above a critical metabolic threshold, as well as a decrease in the incursion of anoxic water masses into the surface ocean and possibly feedbacks of animal evolution onto the environment (51, 52). That is, on the broadest planetary time scale, the physically driven GOE and NOE together appear to have set the timetable of evolution.

Box 1. A simple model for the GOE.

In our deliberately simplified model for the GOE, we consider an ecosystem with two major primary producers: anoxygenic photosynthetic bacteria and cyanobacteria. Anoxygenic photosynthetic bacteria can use a variety of electron donors, but in early oceans, ferrous iron (Fe^{2+}) would have been most important. Cyanobacteria obtain the electrons needed for photosynthesis by splitting water. Anoxygenic photosynthetic bacteria and cyanobacteria compete over the limiting resource, phosphate.

The density of anoxygenic photosynthetic bacteria and cyanobacteria is denoted by x_1 and x_2. Their time derivates are $\dot{x}_1$ and $\dot{x}_2$. Their reproductive rates are r_1 and r_2. Consider the following system of equations

$$\dot{x}_1 = x_1(r_1 z_1 - cx) + u_1$$

$$\dot{x}_2 = x_2(r_2 - cx) + u_2$$

The density-dependent death rate, $-cx$, arises from competition over limiting resources and regulates the total abundance, $x = x_1 + x_2$. We include small migration rates, u_1 and u_2, from ecological niches, where cyanobacteria and anoxygenic photosynthetic bacteria could exist independently of each other.

The reproductive rate of anoxygenic photosynthetic bacteria is multiplied by the concentration of ferrous iron, z_1. As discussed in the main text, oxygen is produced by cyanobacteria and removed by both respiration and geophysical events. For the concentration of oxygen, z_2, we have the equation $\dot{z}_2 = ax_2 - bz_2$, which leads to the steady state $z_2 = ax_2/b$. Thus, the steady-state concentration of oxygen is proportional to the abundance of cyanobacteria. The availability of ferrous iron is reduced by the accumulation of oxygen: For the steady state of ferrous iron, we assume $z_1 = 1/(1 + \alpha z_2)$.

Before the GOE, there is negligible oxygen, and thus, in our model, we have $z_1 \approx 1$. In this case, anoxygenic photosynthetic bacteria dominate the ecosystem provided $r_1 > r_2$. We model the dynamics of the GOE by assuming that the removal rate of oxygen, b, declines over millions of years. The process leads to a slow but continuous increase in the oxygen concentration, slowly reducing the abundance of ferrous iron. There is a sharp transition when the effective growth rate of anoxygenic photosynthetic bacteria becomes less than that of cyanobacteria, $r_1 z_1 < r_2$. At this point, cyanobacteria quickly rise to dominance, which causes oxygen levels to increase markedly. The greatly reduced availability in ferrous iron seals the new world order.

An illustration of the dynamics of the GOE according to this mechanism is shown in the figure below.

Figure: According to our simple model, the dynamics of the GOE is driven by a slow decline in the removal rate of oxygen from the atmosphere due to geophysical events. The accumulation in oxygen causes a reduction in the abundance of ferrous iron, which leads to a sudden dominance of cyanobacteria over anoxygenic photosynthetic bacteria.

Phanerozoic diversification of animals, plants, and protists documents continuing evolutionary innovation and biological interactions, and these, in turn, reflect, at least in part, the continuing influence of planetary change [for example, see the study of Vrba (*186*)], including shifting continents, dynamic climates, and occasional transient geophysical or astrophysical perturbations that drive mass extinctions. Rates of genetic adaptation may be most limiting at the times of rapid and pronounced environmental perturbation that mark mass extinction. As is true for Bacteria and Archaea, a theory explaining the fundamental time scale of evolutionary innovation of eukaryotic organisms remains to be developed. Eukaryotic species have smaller population sizes, longer generation times, and a much diminished capacity for horizontal gene transfer. At the same time, they have distinct mechanisms of genetic regulation, which might both facilitate and constrain the evolution of novel morphologies (*164*, *187*). Evolutionary innovations in plants and animals reflect the accumulation of characters through time and the ecological circumstances under which character change took place (*188*). Angiosperms, for example, postdate the evolution of seed plants by more than 200 million years, their diversification and remarkable ecological success reflecting the developmentally controlled evolution of fruits and accelerated life cycles, as well as functional innovations in leaves and water transport, bolstered by co-evolution with animal pollinators and grazers (*189*). We suspect that, relative to bacteria, evolutionary timing for plants and animals, fungi, and protists will be governed to a greater extent by the accumulation of complex character combinations and other biological factors, including those that help to define the effective environment of populations (this would also be true for younger bacteria, as eukaryotes became important components of their environments). Nonetheless, the fossil record suggests that eukaryotic evolution has continually been influenced by changes in the physical environment, with rates of genetic discovery sufficiently fast to track most geologically resolvable rates of environmental change.

CONCLUSIONS

On billion-year time scales, the evolutionary dynamics of a planet is fast and its evolutionary potential is vast; the pace of evolution is primarily determined by the physical history of the planet. The timetable of evolution, then, is in no small part determined by geophysical events. In the radical formulation of this view, eukaryotes and macroscopic life emerged when the planet was ready for them. Because stars produce specific chemical elements at distinct phases in their life cycles, it could turn out that (a small fraction of) planets produce specific life forms at distinct phases in their evolution. In contrast, on the time scale of transient environmental perturbations such as those associated with the mass extinctions of the last 500 million years, rates of genetic accommodation may be limiting.

In formulating his theory of evolution by natural selection, Charles Darwin (*190*) was inspired by Charles Lyell's *Principles of Geology* (*191*), recognizing in Lyell's view of Earth history the almost limitless expanse of time he thought necessary to understand evolution (*192*). In the 21st century, an increasingly well-resolved timetable of evolution presents opportunities for renewed collaboration between geochronology and evolutionary theory. Resolving the theoretical challenges of evolution's timetable will sharpen our understanding of life's long evolutionary history while informing continuing astrobiological exploration of our own solar system and beyond.

REFERENCES AND NOTES

1. M. J. S. Rudwick, *Earth's Deep History; How It Was Discovered and Why It Matters* (University of Chicago Press, 2014).
2. P. N. Wyse Jackson, John Joly (1857-1933) and his determinations of the age of the Earth. *Geol. Soc. Lond. Spec. Publ.* **190**, 107–119 (2002).
3. D. W. Davis, I. S. Williams, T. E. Krogh, Historical development of zircon geochronology. *Rev. Mineral. Geochem.* **53**, 145–181 (2013).
4. E. S. Barghoorn, S. A. Tyler, Microorganisms from the Gunflint Chert. *Science* **147**, 563–575 (1965).
5. H. L. Allsopp, H. R. Roberts, G. D. L. Schreiner, D. R. Hunter, Rb-Sr age measurements on various Swaziland granites. *J. Geophys. Res.* **67**, 5307–5313 (1962).
6. C. R. Anhaeusser, The evolution of the early Precambrian crust of southern Africa. *Philos. Trans. R. Soc. A Math. Phys. Eng. Sci.* **273**, 359–388 (1973).
7. R. T. Pigeon, 3450-m.y.-old volcanics in Archaean layered greenstone succession of Pilbara Block, Western Australia. *Earth Planet. Sci. Lett.* **37**, 421–428 (1978).
8. T. R. Ireland, S. Clement, W. Compston, J. J. Foster, P. Holden, B. Jenkins, P. Lanc, N. Schram, I. S. Williams, Development of SHRIMP. *Aust. J. Earth Sci.* **5**, 937–954 (2008).
9. N. J. McNaughton, W. Compston, M. E. Barley, Constraints on the age of the Warrawoona Group, eastern Pilbara Block, Western Australia. *Precambrian Res.* **60**, 69–98 (1993).
10. M. J. Van Kranendonk, A. H. Hickman, R. S. Smithies, D. R. Nelson, G. Pike, Geology and tectonic evolution of the Archaean North Pilbara Terrain, Pilbara Craton, Western Australia. *Econ. Geol.* **97**, 695–732 (2002).
11. A. C. Allwood, M. R. Walter, B. S. Kamber, C. P. Marshall, I. W. Burch, Stromatolite reef from the Early Archaean era of Australia. *Nature* **441**, 714–718 (2006).
12. A. C. Allwood, J. P. Grotzinger, A. H. Knoll, I. W. Burch, M. S. Anderson, M. L. Coleman, I. Kanik, Controls on development and diversity of Early Archean stromatolites. *Proc. Natl. Acad. Sci. U.S.A.* **106**, 9548–9555 (2009).
13. J.-P. Duda, M. J. van Kranendonk, V. Thiel, D. Ionescu, H. Strauss, N. Schäfer, J. Reitner, A rare glimpse of Paleoarchean life: Geobiology of an exceptionally preserved microbial mat facies from the 3.4 Ga Strelley Pool Formation, Western Australia. *PLOS ONE* **11**, e0147629 (2016).
14. D. R. Nelson, Compilation of geochronology data, June 2005 update (Geological Survey of Western Australia, 2005).
15. S. W. Awramik, J. W. Schopf, M. R. Walter, Filamentous fossil bacteria from the Archean of Western Australia. *Precambrian Res.* **20**, 357–374 (1983).
16. J. W. Schopf, Microfossils of the Early Archean Apex chert: New evidence of the antiquity of life. *Science* **260**, 640–646 (1993).
17. K. Sugitani, K. Lepot, T. Nagaoka, K. Mimura, M. van Kranendonk, D. Z. Oehler, M. R. Walter, Biogenicity of morphologically diverse carbonaceous microstructures from the ca. 3400 Ma Strelley Pool Formation, in the Pilbara Craton, Western Australia. *Astrobiology* **10**, 899–920 (2010).
18. M. D. Brasier, O. R. Green, J. F. Lindsay, N. McLoughlin, A. Steele, C. Stoakes, Critical testing of Earth's oldest putative fossil assemblage from the similar to ~3.5 Ga Apex Chert, Chinaman Creek, Western Australia. *Precambrian Res.* **140**, 55–102 (2005).
19. D. Wacey, *Early Life on Earth: A Practical Guide* (Springer, 2009).
20. A. H. Knoll, K. Bergmann, J. V. Strauss, Life: The first two billion years. *Philos. Trans. R. Soc. B Biol. Sci.* **371**, 20150493 (2016).
21. J. W. Schopf, Fossil evidence of Archean life. *Philos. Trans. R. Soc. Lond. B. Biol. Sci.* **361**, 861–885 (2006).
22. T. R. R. Bontognali, A. L. Sessions, A. C. Allwood, W. W. Fischer, J. P. Grotzinger, R. E. Summons, J. M. Eiler, Sulfur isotopes of organic matter preserved in 3.45-billion-year-old stromatolites reveal microbial metabolism. *Proc. Natl. Acad. Sci. U.S.A.* **109**, 15146–15151 (2013).
23. S. L. Kamo, D. L. Davis, Reassessment of Archean crustal development in the Barberton Mountain Land, South Africa, based on U-Pb dating. *Tectonics* **13**, 167–192 (1994).
24. M. T. Rosing, ¹³C-depleted carbon microparticles in >3700-Ma sea-floor sedimentary rocks from west Greenland. *Science* **283**, 674–676 (1999).
25. A. P. Nutman, V. C. Bennett, C. R. L. Friend, M. L. Van Kranendonk, A. R. Chivas, Rapid emergence of life shown by discovery of 3,700-million-year-old microbial structures. *Nature* **537**, 535–538 (2016).
26. E. A. Bell, P. Boehnke, T. M. Harrison, W. L. Mao, Potentially biogenic carbon preserved in a 4.1 billion-year-old zircon. *Proc. Natl. Acad. Sci. U.S.A.* **112**, 14518–14521 (2015).
27. H. D. Holland, The oxygenation of the atmosphere and oceans. *Philos. Trans. R. Soc. Lond. B. Biol. Sci.* **361**, 903–915 (2006).
28. A. Bekker, H. D. Holland, P.-L. Wang, D. Rumble III, H. J. Stein, J. L. Hannah, L. I. Coetzee, N. J. Beukes, Dating the rise of atmospheric oxygen. *Nature* **427**, 117–120 (2004).
29. J. E. Johnson, A. Gerpheide, M. P. Lamb, W. W. Fischer, O₂ constraints from Paleoproterozoic detrital pyrite and uraninite. *Geol. Soc. Am. Bull.* **126**, 813–830 (2014).
30. A. P. Gumsley, K. R. Chamberlain, W. Bleeker, U. Söderlund, M. O. de Kock, E. R. Larsson, A. Bekker, Timing and tempo of the great oxidation event. *Proc. Natl. Acad. Sci. U.S.A.* **114**, 1811–1816 (2017).

31. J. Raymond, D. Segré, The effect of oxygen on biochemical networks and the evolution of complex life. *Science* **311**, 1764–1767 (2006).

32. D. M. Lamb, S. M. Awramik, D. J. Chapman, S. Zhu, Evidence for eukaryotic diversification in the similar to ~1800 million-year-old Changzhougou Formation, North China. *Precambrian Res.* **173**, 93–104 (2009).

33. H. Li, S. Lu, W. Su, Z. Xiang, H. Zhou, Y. Zhang, Recent advances in the study of the Mesoproterozoic geochronology in the North China Craton. *J. Asian Earth Sci.* **72**, 216–227 (2013).

34. E. J. Javaux, A. H. Knoll, Micropaleontology of the lower Mesoproterozoic Roper Group, Australia, and implications for early eukaryotic evolution. *J. Paleontol.* **91**, 199–229 (2017).

35. M. R. Walter, R. Du, R. J. Horodyski, Coiled carbonaceous megafossils from the Middle Proterozoic of Jixian (Tianjin) and Montana. *Am. J. Sci.* **290A**, 133–148 (1990).

36. S. Zhu, S. M. Zhu, A. H. Knoll, Z. Yin, F. Zhao, S. Sun, Y. Qu, M. Shi, H. Liu, Decimetre-scale multicellular eukaryotes from the 1.56-billion-year-old Gaoyuzhuang Formation in North China. *Nat. Commun.* **7**, 11500 (2016).

37. N. J. Butterfield, *Bangiomorpha pubescens* n. gen., n. sp.: Implications for the evolution of sex, multicellularity, and the Mesoproterozoic/Neoproterozoic radiation of eukaryotes. *Paleobiology* **26**, 386–404 (2000).

38. S. M. Porter, R. Meisterfeld, A. H. Knoll, Vase-shaped microfossils from the Neoproterozoic Chuar Group, Grand Canyon: A classification guided by modern testate amoebae. *J. Paleontol.* **77**, 409–429 (2003).

39. P. A. Cohen, A. H. Knoll, Neoproterozoic scale microfossils from the Fifteen Mile Group, Yukon Territory. *J. Paleontol.* **86**, 775–800 (2012).

40. N. J. Butterfield, Reconstructing a complex Early Neoproterozoic eukaryote, Wynniatt Formation, Arctic Canada. *Lethaia* **38**, 155–169 (2005).

41. N. J. Butterfield, A. H. Knoll, K. Swett, Paleobiology of the upper Proterozoic Svanbergfjellet Formation, Spitsbergen. *Fossils Strata* **34**, 1–84 (1994).

42. F. A. Macdonald, M. D. Schmitz, J. L. Crowley, C. F. Roots, D. S. Jones, A. C. Maloof, J. V. Strauss, P. A. Cohen, D. T. Johnston, D. P. Schrag, Calibrating the Cryogenian. *Science* **327**, 1241–1243 (2010).

43. J. V. Strauss, A. D. Rooney, F. A. Macdonald, A. D. Brandon, A. H. Knoll, Circa 740 Ma vase-shaped microfossils from the Yukon Territory: Implications for Neoproterozoic biostratigraphy. *Geology* **42**, 659–662 (2014).

44. D. H. Erwin, M. Laflamme, S. M. Tweedt, E. A. Sperling, D. Pisani, K. J. Peterson, The Cambrian conundrum: Early divergence and later ecological success in the early history of animals. *Science* **334**, 1091–1097 (2011).

45. L. M. Och, G. A. Shields-Zhou, The Neoproterozoic oxygenation event: Environmental perturbations and biogeochemical cycling. *Earth Sci. Rev.* **110**, 26–57 (2012).

46. P. A. E. P. von Strandmann, E. E. Stüeken, T. Elliott, S. W. Poulton, C. M. Dehler, D. E. Canfield, C. Catling, Selenium isotope evidence for progressive oxidation of the Neoproterozoic biosphere. *Nat. Commun.* **6**, 10157 (2015).

47. S. K. Sahoo, N. J. Planavsky, B. Kendall, X. Wang, X. Shi, C. Scott, A. D. Anbar, T. W. Lyons, G. Jiang, Ocean oxygenation in the wake of the Marinoan glaciation. *Nature* **489**, 546–549 (2012).

48. T. W. Dahl, E. Hammarlund, B. C. Gill, A. H. Knoll, A. D. Anbar, G. W. Gordon, D. P. G. Bond, N. H. Schovsbo, A. T. Nielsen, D. E. Canfield, Devonian rise in atmospheric oxygen correlated to the radiations of terrestrial plants and large predatory fish. *Proc. Natl. Acad. Sci. U.S.A.* **107**, 17911–17915 (2010).

49. E. A. Sperling, C. J. Wolock, A. S. Morgan, B. C. Gill, M. Kunzmann, G. P. Halverson, F. A. Macdonald, A. H. Knoll, D. T. Johnston, Statistical analysis of iron geochemical data suggests limited late Proterozoic oxygenation. *Nature* **523**, 451–454 (2015).

50. S. K. Sahoo, N. J. Planavsky, G. Jiang, B. Kendall, J. D. Owens, X. Wang, X. Shi, A. D. Anbar, T. W. Lyons, Oceanic oxygenation events in the anoxic Ediacaran ocean. *Geobiology* **14**, 457–468 (2016).

51. E. A. Sperling, A. H. Knoll, P. R. Girguis, The ecological physiology of Earth's second oxygen revolution. *Annu. Rev. Ecol. Evol. Syst.* **46**, 215–235 (2015).

52. T. M. Lenton, R. A. Boyle, S. W. Poulton, G. A. Shields-Zhou, N. J. Butterfield, Co-evolution of eukaryotes and ocean oxygenation in the Neoproterozoic era. *Nat. Geosci.* **7**, 257–265 (2014).

53. R. R. Parrish, S. R. Noble, Zircon U-Th-Pb geochronology by isotope dilution–thermal ionization mass spectrometry (ID-TIMS). *Rev. Mineral. Geochem.* **53**, 183–213 (2003).

54. S. A. Bowring, J. P. Grotzinger, C. E. Isachsen, A. H. Knoll, S. M. Pelechaty, P. Kolosov, Calibrating rates of early Cambrian evolution. *Science* **261**, 1293–1298 (1993).

55. S. A. Bowring, J. P. Grotzinger, D. J. Condon, J. Ramezani, M. J. Newall, P. A. Allen, Geochronologic constraints on the chronostratigraphic framework of the Neoproterozoic Huqf Supergroup, Sultanate of Oman. *Am. J. Sci.* **307**, 1097–1145 (2007).

56. J. P. Grotzinger, S. A. Bowring, B. Z. Saylor, A. J. Kaufman, Biostratigraphic and geochronologic constraints on early animal evolution. *Science* **270**, 598–604 (1995).

57. M. Zhou, T. Luo, S. Liu, Z. Qian, L. Xing, SHRIMP zircon age for a K-bentonite in the top of the Laobao Formation at the Pingyin section, Guizhou, South China. *Sci. China Earth Sci.* **56**, 1677–1687 (2013).

58. A. C. Maloof, S. M. Porter, J. L. Moore, F. Dudás, S. A. Bowring, J. A. Higgins, D. A. Fike, M. P. Eddy, The earliest Cambrian record of animals and ocean geochemical change. *Geol. Soc. Am. Bull.* **122**, 1731–1774 (2010).

59. E. D. Landing, G. Geyer, R. Buchwaldt, S. A. Bowring, Geochronology of the Cambrian: A precise Middle Cambrian U–Pb zircon date from the German margin of West Gondwana. *Geol. Mag.* **152**, 28–40 (2014).

60. S. Conway Morris, J. S. Peel, A. K. Higgins, N. J. Soper, N. C. Davis, A Burgess shale-like fauna from the Lower Cambrian of North Greenland. *Nature* **326**, 181–183 (1987).

61. J.Y. Chen, G.Q. Zhou, M.Y. Zhu, K.Y. Yeh, *The Chengjiang Biota: A Unique Window of the Cambrian Explosion* (National Museum of Natural Science, 1997).

62. J. R. Paterson, D. C. García-Bellido, J. B. Jago, J. G. Gehling, M. S. Y. Lee, G. D. Edgecombe, The Emu Bay Shale Konservat-Lagerstätte: A view of Cambrian life from East Gondwana. *J. Geol. Soc.* **173**, 1–11 (2016).

63. T. H. P. Harvey, M. Williams, D. J. Condon, P. R. Wilby, D. J. Siveter, A. W. A. Rushton, M. J. Leng, S. E. Gabbott, A refined chronology for the Cambrian succession of southern Britain. *J. Geol. Soc.* **168**, 705–716 (2011).

64. G. E. Budd, S. Jensen, A critical reappraisal of the fossil record of the bilaterian phyla. *Biol. Rev.* **75**, 253–295 (2000).

65. J. P. Pu, S. A. Bowring, J. Ramezani, P. Myrow, T. D. Raub, E. Landing, A. Mills, E. Hodgin, F. A. Macdonald, Dodging snowballs: Geochronology of the Gaskiers glaciation and the first appearance of the Ediacaran biota. *Geology* **44**, 955–958 (2016).

66. A. G. Liu, D. McIlroy, M. D. Brasier, First evidence for locomotion in the Ediacara biota from the 565 Ma Mistaken Point Formation, Newfoundland. *Geology* **38**, 123–126 (2010).

67. M. W. Martin, D. V. Grazhdankin, S. A. Bowring, D. A. D. Evans, M. A. Fedonkin, J. L. Kirschvink, Age of Neoproterozoic bilaterian body and trace fossils, White Sea, Russia: Implications for Metazoan evolution. *Science* **288**, 841–845 (2000).

68. D. Grazhdankin, Patterns of evolution of the Ediacaran soft-bodied biota. *J. Paleontol.* **88**, 269–283 (2014).

69. M. Moczydłowska, G. E. Budd, H. Agić, Ecdysozoan-like sclerites among Ediacaran microfossils. *Geol. Mag.* **152**, 1145–1148 (2015).

70. M. D. Schmitz, Radiometric ages used in GTS2012, in *The Geologic Time Scale 2012*, F. M. Gradstein, J. G. Ogg, M. Schmitz, G. Ogg, Eds. (Elsevier, 2012), pp. 1045–1082.

71. J. M. Husson, B. Schoene, S. Bluher, A. C. Maloof, Chemostratigraphic and U–Pb geochronologic constraints on carbon cycling across the Silurian–Devonian boundary. *Earth Planet. Sci. Lett.* **436**, 108–120 (2016).

72. B. Kaufmann, E. Trapp, K. Mezger, The numerical age of the Upper Frasnian (Upper Devonian) Kellwasser horizons: A new U-Pb zircon date from Steinbruch Schmidt (Kellerwald, Germany). *J. Geol.* **112**, 495–501 (2004).

73. P. Gensel, The earliest land plants. *Annu. Rev. Ecol. Evol. Syst.* **39**, 459–477 (2008).

74. P. K. Strother, G. D. Wood, W. A. Taylor, J. H. Beck, Middle Cambrian cryptospores and the origin of land plants. *Assoc. Australas. Palaeontol. Mem.* **29**, 99–113 (2004).

75. D. Edwards, Xylem in early tracheophytes. *Plant Cell Environ.* **26**, 57–72 (2003).

76. D. Edwards, Embryophytic sporophytes in the Rhynie and Windyfield cherts. *Trans. R. Soc. Edinb. Earth Sci.* **94**, 397–410 (2004).

77. D. F. Mark, C. M. Rice, A. E. Fallick, N. H. Trewin, M. R. Lee, A. Boyce, J. K. W. Lee, [40]Ar/[39]Ar dating of hydrothermal activity, biota and gold mineralization in the Rhynie hot-spring system, Aberdeenshire, Scotland. *Geochim. Cosmochim. Acta* **75**, 555–569 (2011).

78. J. A. Dunlop, Geological history and phylogeny of Chelicerata. *Arthropod Struct. Dev.* **39**, 124–142 (2010).

79. W. A. Shear, G. D. Edgecombe, The geological record and phylogeny of the Myriapoda. *Arthropod Struct. Dev.* **39**, 174–190 (2010).

80. M. S. Engel, D. A. Grimaldi, New light shed on the oldest insect. *Nature* **427**, 627–630 (2004).

81. E. B. Daeschler, N. H. Shubin, F. A. Jenkins Jr., A Devonian tetrapod-like fish and the evolution of the tetrapod body plan. *Nature* **440**, 757–763 (2006).

82. J.A. Clack, *Gaining Ground: The Origin and Evolution of Tetrapods* (Indiana Univ. Press, ed. 2, 2012).

83. S. Katoh, Y. Beyene, T. Itaya, H. Hyodo, M. Hyodo, K. Yagi, C. Gouzu, G. WoldeGabriel, W. K. Hart, S. H. Ambrose, H. Nakaya, R. L. Bernor, J.-R. Boisserie, F. Bibi, H. Saegusa, T. Sasaki, K. Sano, B. Asfaw, G. Suwa, New geological and palaeontological age constraint for the gorilla–human lineage split. *Nature* **530**, 215–218 (2016).

84. B. Villmoare, W. H. Kimbel, C. Seyoum, C. J. Campisano, E. N. Di Maggio, J. Rowan, D. R. Braun, J. R. Arrowsmith, K. E. Reed, Early *Homo* at 2.8 Ma from Ledi-Geraru, Afar, Ethiopia. *Science* **347**, 1352–1355 (2015).

85. J. H. Schwartz, I. Tattersall, Defining the genus *Homo*. *Science* **349**, 931–932 (2015).

86. I. McDougall, F. H. Brown, P. M. Vasconcelos, B. E. Cohen, D. S. Thiede, M. J. Buchanan, New single crystal [40]Ar/[39]Ar ages improve time scale for deposition of the Omo Group, Omo–Turkana Basin, East Africa. *J. Geol. Soc.* **169**, 213–226 (2012).

87. C. J. Lepre, Early Pleistocene lake formation and hominin origins in the Turkana-Omo rift. *Quat. Sci. Rev.* **102**, 181–191 (2014).

88. Y. Beyene, S. Katoh, G. WoldeGabriel, W. K. Hart, K. Uto, M. Sudo, M. Kondo, M. Hyodo, P. R. Renne, G. Suwa, B. Asfaw, The characteristics and chronology of the earliest Acheulean at Konso, Ethiopia. *Proc. Nat. Acad. Sci. U.S.A.* **110**, 1584–1591 (2013).

89. C. J. Lepre, D. V. Kent, New magnetostratigraphy for the Olduvai Subchron in the Koobi Fora Formation, northwest Kenya, with implications for early Homo. *Earth Planet. Sci. Lett.* **290**, 362–374 (2010).

90. R. Ferring, O. Oms, J. Agustí, F. Berna, M. Nioradze, T. Shelia, M. Tappen, A. Vekua, D. Zhvania, D. Lordkipanidze, Earliest human occupations at Dmanisi (Georgian Caucasus) dated to 1.85–1.78 Ma. *Proc. Natl. Acad. Sci. U.S.A.* **108**, 10432–10436 (2011).

91. I. McDougall, F. H. Brown, J. G. Fleagle, Stratigraphic placement and age of modern humans from Kibish, Ethiopia. *Nature* **433**, 733–736 (2005).

92. M. Grove, Palaeoclimates, plasticity, and the early dispersal of *Homo sapiens*. *Quat. Int.* **369**, 17–37 (2015).

93. S. Mallick, H. Li, M. Lipson, I. Mathieson, M. Gymrek, F. Racimo, M. Zhao, N. Chennagiri, S. Nordenfelt, A. Tandon, P. Skoglund, I. Lazaridis, S. Sankararaman, Q. Fu, N. Rohland, G. Renaud, Y. Erlich, T. Willems, C. Gallo, J. P. Spence, Y. S. Song, G. Poletti, F. Balloux, G. van Driem, P. de Knijff, I. G. Romero, A. R. Jha, D. M. Behar, C. M. Bravi, C. Capelli, T. Hervig, A. Moreno-Estrada, O. L. Posukh, E. Balanovska, O. Balanovsky, S. Karachanak-Yankova, H. Sahakyan, D. Toncheva, A. Tyler-Smith, Y. Xue, M. S. Abdullah, A. Ruiz-Linares, C. M. Beall, A. Di Rienzo, C. Jeong, E. B. Starikovskaya, E. Metspalu, J. Parik, R. Villems, B. M. Henn, U. Hodoglugil, R. Mahley, A. Sajantila, G. Stamatoyannopoulos, J. T. S. Wee, R. Khusainova, E. Khusnutdinova, S. Litvinov, G. Ayodo, D. Comas, M. F. Hammer, T. Kivisild, W. Klitz, C. A. Winkler, D. Labuda, M. Bamshad, L. B. Jorde, S. A. Tishkoff, W. Scott Watkins, M. Metspalu, S. Dryomov, R. Sukernik, L. Singh, K. Thangaraj, S. Pääbo, J. Kelso, N. Patterson, D. Reich, The Simons Genome Diversity Project: 300 genomes from 142 diverse populations. *Nature* **538**, 201–206 (2016).

94. A.-S. Malaspinas, M. C. Westaway, C. Muller, V. C. Sousa, O. Lao, I. Alves, A. Bergström, G. Athanasiadis, J. Y. Cheng, J. E. Crawford, T. H. Heupink, E. Macholdt, S. Peischl, S. Rasmussen, S. Schiffels, S. Subramanian, J. L. Wright, A. Albrechtsen, C. Barbieri, I. Dupanloup, A. Eriksson, A. Margaryan, I. Moltke, I. Pugach, T. S. Korneliussen, I. P. Levkivskyi, J. Víctor Moreno-Mayar, S. Ni, F. Racimo, M. Sikora, Y. Xue, F. A. Aghakhanian, N. Brucato, S. Brunak, P. F. Campos, W. Clark, S. Ellingvåg, G. Fourmile, P. Gerbault, D. Injie, G. Koki, M. Leavesley, B. Logan, A. Lynch, E. A. Matisoo-Smith, P. J. McAllister, A. J. Mentzer, M. Metspalu, A. B. Migliano, L. Murgha, M. E. Phipps, W. Pomat, D. Reynolds, F.-X. Ricaut, P. Siba, M. G. Thomas, T. Wales, C. Wall, S. J. Oppenheimer, C. Tyler-Smith, R. Durbin, J. Dortch, A. Manica, M. H. Schierup, R. A. Foley, M. M. Lahr, C. Bowern, J. D. M. Wall, T. Mailund, M. Stoneking, R. Nielsen, M. S. Sandhu, L. Excoffier, D. M. Lambert, E. Willerslev, A genomic history of Aboriginal Australia. *Nature* **538**, 207–214 (2016).

95. L. Pagani, D. J. Lawson, E. Jagoda, A. Mörseburg, A. Eriksson, M. Mitt, F. Clemente, G. Hudjashov, M. DeGiorgio, L. Saag, J. D. Wall, A. Cardona, R. Mägi, M. A. Wilson Sayres, S. Kaewert, C. Inchley, C. L. Scheib, M. Järve, M. Karmin, G. S. Jacobs, T. Antao, F. M. Iliescu, A. Kushniarevich, Q. Ayub, C. Tyler-Smith, Y. Xue, B. Yunusbayev, K. Tambets, C. B. Mallick, L. Saag, E. Pocheshkhova, G. Andriadze, C. Muller, M. C. Westaway, D. M. Lambert, G. Zoraqi, S. Turdikulova, D. Dalimova, Z. Sabitov, G. N. N. Sultana, J. Lachance, S. Tishkoff, K. Momynaliev, J. Isakova, L. D. Damba, M. Gubina, P. Nymadawa, I. Evseeva, L. Atramentova, O. Utevska, F.-X. Ricaut, N. Brucato, H. Sudoyo, T. Letellier, M. P. Cox, N. A. Barashkov, V. Škaro, L. Mulahasanović, D. Primorac, H. Sahakyan, M. Mormina, C. A. Eichstaedt, D. V. Lichman, S. Abdullah, G. Chaubey, J. T. S. Wee, E. Mihailov, A. Karunas, S. Litvinov, R. Khusainova, N. Ekomasova, V. Akhmetova, I. Khidiyatova, D. Marjanović, L. Yepiskoposyan, D. M. Behar, E. Balanovska, A. Metspalu, M. Derenko, B. Malyarchuk, M. Voevoda, S. A. Fedorova, L. P. Osipova, M. M. Lahr, P. Gerbault, M. Leavesley, A. B. Migliano, M. Petraglia, O. Balanovsky, E. K. Khusnutdinova, E. Metspalu, M. G. Thomas, A. Manica, R. Nielsen, R. Villems, E. Willerslev, T. Kivisild, M. Metspalu, Genomic analyses inform on migration events during the peopling of Eurasia. *Nature* **538**, 238–242 (2016).

96. F. M. Gradstein, J. G. Ogg, Geologic Time Scale 2004—Why, how, and where next! *Lethaia* **37**, 175–181 (2004).

97. H. Hercman, J. Pawlak, StronTer: Tools for probabilistic methods in strontium isotope stratigraphy. *J. Geol.* **124**, 267–275 (2016).

98. J. Phillips, *Life on the Earth: Its Origin and Succession* (MacMillan, 1860).

99. L. W. Alvarez, W. Alvarez, F. Asaro, H. V. Michel, Extraterrestrial cause for the Cretaceous-Tertiary extinction: Experimental results and theoretical interpretation. *Science* **208**, 1095–1108 (1980).

100. P. Schulte, L. Alegret, I. Arenillas, J. A. Arz, P. J. Barton, P. R. Bown, T. J. Bralower, G. L. Christeson, P. Claeys, C. S. Cockell, G. S. Collins, A. Deutsch, T. J. Goldin, K. Goto, J. M. Grajales-Nishimura, R. A. F. Grieve, S. P. S. Gulick, K. R. Johnson, W. Kiessling, C. Koeberl, D. A. Kring, K. G. MacLeod, T. Matsui, J. Melosh, A. Montanari, J. V. Morgan, C. R. Neal, D. J. Nichols, R. D. Norris, E. Pierazzo, G. Ravizza, M. Rebolledo-Vieyra, W. Uwe Reimold, E. Robin, T. Salge, R. P. Speijer, A. R. Sweet, J. Urrutia-Fucugauchi, V. Vajda, M. T. Whalen, P. S. Willumsen, The Chicxulub asteroid impact and mass extinction at the Cretaceous-Paleogene boundary. *Science* **327**, 1214–1218 (2010).

101. P. R. Renne, A. L. Deino, F. J. Hilgen, K. F. Kuiper, D. F. Mark, W. S. Mitchell III, L. E. Morgan, R. Mundil, J. Smit, Time scales of critical events around the Cretaceous-Paleogene boundary. *Science* **339**, 684–687 (2013).

102. B. Schoene, K. M. Samperton, M. P. Eddy, G. Keller, T. Adatte, S. A. Bowring, S. F. R. Khadri, B. Gertsch, U-Pb geochronology of the Deccan Traps and relation to the end-Cretaceous mass extinction. *Science* **347**, 182–184 (2015).

103. M. A. Richards, W. Alvarez, S. Self, L. Karlstrom, P. R. Renne, M. Manga, C. J. Sprain, J. Smit, L. Vanderkluysen, S. A. Gibson, Triggering of the largest Deccan eruptions by the Chicxulub impact. *Geol. Soc. Am. Bull.* **127**, 1507–1520 (2015).

104. R. K. Bambach, Phanerozoic biodiversity mass extinctions. *Annu. Rev. Earth Planet. Sci.* **34**, 127–155 (2006).

105. S. D. Burgess, S. A. Bowring, S. Shen, High-precision timeline for Earth's most severe extinction. *Proc. Natl. Acad. Sci. U.S.A.* **111**, 3316–3321 (2014).

106. S. D. Burgess, S. A. Bowring, High-precision geochronology confirms voluminous magmatism before, during, and after Earth's most severe extinction. *Sci. Adv.* **1**, e1500470 (2015).

107. D. H. Erwin, Temporal acuity and the rate and dynamics of mass extinctions. *Proc. Nat. Acad. Sci. U.S.A.* **111**, 3203–3204 (2014).

108. A. H. Knoll, R. K. Bambach, J. L. Payne, S. Pruss, W. W. Fischer, Paleophysiology and end-Permian mass extinction. *Earth Planet. Sci. Lett.* **256**, 295–313 (2007).

109. B. Hönisch, A. Ridgwell, D. N. Schmidt, E. Thomas, S. J. Gibbs, A. Sluijs, R. Zeebe, L. Kump, R. C. Martindale, S. E. Greene, W. Kiessling, J. Ries, J. C. Zachos, D. L. Royer, S. Barker, T. M. Marchitto Jr., R. Moyer, C. Pelejero, P. Ziveri, G. L. Foster, B. Williams, The geological record of ocean acidification. *Science* **335**, 1058–1063 (2012).

110. B. van de Schootbrugge, P. B. Wignall, A tale of two extinctions: Converging end-Permian and end-Triassic scenarios. *Geol. Mag.* **153**, 332–354 (2016).

111. S. D. Burgess, S. A. Bowring, T. H. Fleming, D. H. Elliot, High-precision geochronology links the Ferrar large igneous province with early-Jurassic ocean anoxia and biotic crisis. *Earth Planet. Sci. Lett.* **415**, 90–99 (2015).

112. R. Zeebe, A. Ridgwell, J. C. Zachos, Anthropogenic carbon release rate unprecedented during the past 66 million years. *Nat. Geosci.* **9**, 325–329 (2016).

113. G.G. Simpson, *Tempo and Mode in Evolution* (Columbia Univ. Press, 1944).

114. G.G. Simpson, *The Major Features of Evolution* (Columbia Univ. Press, 1953).

115. S. A. Bowring, D. H. Erwin, A new look at evolutionary rates in deep time: Uniting paleontology and high-precision geochronology. *GSA Today* **8**, 1–8 (1998).

116. G. Hunt, D. L. Rabosky, Phenotypic evolution in fossil species: Pattern and process. *Annu. Rev. Earth Planet. Sci.* **42**, 421–441 (2014).

117. G. Hunt, M. J. Hopkins, S. Lidgard, Simple versus complex models of trait evolution and stasis as a response to environmental change. *Proc. Natl. Acad. Sci. U.S.A.* **112**, 4885–4890 (2015).

118. S. M. Stanley, Rates of evolution. *Paleobiology* **11**, 13–26 (1985).

119. P. D. Gingerich, Rates of evolution: Effects of time and temporal scaling. *Science* **222**, 159–161 (1983).

120. P. D. Gingerich, Rates of evolution on the time scale of the evolutionary process. *Genetica* **112–113**, 127–144 (2001).

121. S. J. Gould, Smooth curve of evolutionary rate—A psychological and mathematical artifact. *Science* **226**, 994–996 (1984).

122. D. M. Raup, R. E. Crick, Evolution of single characters in the Jurassic ammonite *Kosmoceras*. *Paleobiology* **7**, 200–215 (1981).

123. P. M. Sadler, Sediment accumulation rates and the completeness of stratigraphic sections. *J. Geol.* **89**, 569–584 (1981).

124. T. S. Westoll, On the evolution of the Dipnoi, in *Genetics, Paleontology and Evolution*, G. L. Jepsen, G. G. Simpson, E. Mayr, Eds. (Princeton Univ. Press, 1949), pp. 121–184.

125. G. T. Lloyd, Estimating morphological diversity and tempo with discrete character-taxon matrices: Implementation, challenges, progress, and future directions. *Biol. J. Linn. Soc.* **118**, 131–151 (2016).

126. M. J. Hopkins, A. M. Smith, Dynamic evolutionary change in post-Paleozoic echinoids and the importance of scale when interpreting changes in rates of evolution. *Proc. Nat. Acad. Sci. U.S.A.* **112**, 3758–3763 (2015).

127. D. E. G. Briggs, R. A. Fortey, M. A. Wills, Morphological disparity in the Cambrian. *Science* **256**, 1670–1673 (1992).

128. M. Foote, Morphological disparity in Ordovician-Devonian crinoids and the early saturation of morphological space. *Paleobiology* **20**, 320–344 (1994).

129. C. K. Boyce, A. H. Knoll, Evolution of developmental potential and the multiple independent origins of leaves in Paleozoic vascular plants. *Paleobiology* **28**, 70–100 (2002).

130. B. Kotrc, A. H. Knoll, A morphospace of planktonic marine diatoms. I. Two views of disparity through time. *Paleobiology* **41**, 45–67 (2015).

131. M. Foote, The evolution of morphological diversity. *Annu. Rev. Ecol. Syst.* **128**, 129–152 (1997).

132. M. J. Hopkins, Magnitude versus direction of change and the contribution of macroevolutionary trends to morphological disparity. *Biol. J. Linnean. Soc.* **118**, 116–130 (2016).

133. C. Mitter, B. Farrell, B. Wiegmann, The phylogenetic study of adaptive zones: Has phytophagy promoted insect diversification? *Am. Nat.* **132**, 107–128 (1988).

134. S. Magallón, M. J. Sanderson, Absolute diversification rates in angiosperm clades. *Evolution* **55**, 1762–1780 (2001).

135. J. J. Sepkoski Jr., A factor analytic description of the Phanerozoic marine fossil record. *Paleobiology* **7**, 36–53 (1981).

136. J. J. Sepkoski Jr., Rates of speciation in the fossil record. *Philos. Trans. R. Soc. Lond. B Biol. Sci.* **353**, 315–326 (1998).

137. M. Foote, Survivorship analysis of Cambrian and Ordovician trilobites. *Paleobiology* **14**, 258–271 (1988).

138. M. Webster, A Cambrian peak in morphological variation within species. *Science* **317**, 499–502 (2007).

139. N. L. Gilinsky, R. K. Bambach, Asymmetrical patterns of origination and extinction in higher taxa. *Paleobiology* **13**, 427–445 (1987).

140. D. L. Rabosky, A. H. Hurlbert, Species richness at continental scales is dominated by ecological limits. *Am. Nat.* **185**, 572–583 (2015).

141. A. M. Bush, G. Hunt, R. K. Bambach, Sex and the shifting biodiversity dynamics of marine animals in deep time. *Proc. Nat. Acad. Sci. U.S.A.* **113**, 14073–14078 (2016).

142. A.H. Knoll, Patterns of change in plant communities through geologic time, in *Community Ecology*, T. Case, J. Diamond, Eds. (Harper and Row, 1986), pp. 126–141.

143. C. R. Marshall, T. B. Quental, The uncertain role of diversity dependence in species diversification and the need to incorporate time-varying carrying capacities. *Philos. Trans. R. Soc. Lond. B Biol. Sci.* **371**, 20150217 (2016).

144. T. H. G. Ezard, A. Purvis, Environmental changes define ecological limits to species richness and reveal the mode of macroevolutionary competition. *Ecol. Lett.* **19**, 899–906 (2016).

145. B. E. Schirrmeister, M. Gugger, P. C. J. Donoghue, Cyanobacteria and the Great Oxidation Event: Evidence from genes and fossils. *Palaeontology* **58**, 769–785 (2015).

146. L. W. Parfrey, D. J. G. Lahr, A. H. Knoll, L. A. Katz, Estimating the timing of early eukaryotic diversification with multigene molecular clocks. *Proc. Nat. Acad. Sci. U.S.A.* **108**, 13624–13629 (2011).

147. L. Eme, S. C. Sharpe, M. W. Brown, A. J. Roger, On the age of eukaryotes: Evaluating evidence from fossils and molecular clocks. *Cold Spring Harb. Perspect. Biol.* **6**, a016139 (2014).

148. E. Biffin, T. J. Brodribb, R. S. Hill, P. Thomas, A. J. Lowe, Leaf evolution in Southern Hemisphere conifers tracks the angiosperm ecological radiation. *Proc. Biol. Sci.* **279**, 341–348 (2012).

149. R. W. Meredith, J. E. Janečka, J. Gatesy, O. A. Ryder, C. A. Fisher, E. C. Teeling, A. Goodbla, E. Eizirik, T. L. L. Simão, T. Stadler, D. L. Rabosky, R. L. Honeycutt, J. J. Flynn, C. M. Ingram, C. Steiner, T. L. Williams, T. J. Robinson, A. Burk-Herrick, M. Westerman, N. A. Ayoub, M. S. Springer, W. J. Murphy, Impacts of the Cretaceous terrestrial revolution and KPg extinction on mammal diversification. *Science* **334**, 521–524 (2011).

150. T. H. G. Ezard, G. H. Thomas, A. Purvis, Inclusion of a near-complete fossil record reveals speciation-related molecular evolution. *Methods Ecol. Evol.* **4**, 745–753 (2013).

151. A. H. Knoll, Proterozoic and Early Cambrian protists: Evidence for accelerating evolutionary tempo. *Proc. Nat. Acad. Sci. U.S.A.* **91**, 6743–6750 (1994).

152. N. J. Butterfield, Plankton ecology and the Proterozoic-Phanerozoic transition. *Paleobiology* **23**, 247–262 (1997).

153. E. Szathmáry, Toward major evolutionary transitions theory 2.0. *Proc. Nat. Acad. Sci. U.S.A.* **112**, 10104–10111 (2015).

154. M. A. O'Malley, R. Powell, Major problems in evolutionary transitions: How a metabolic perspective can enrich our understanding of macroevolution. *Biol. Philos.* **31**, 159–169 (2016).

155. M.A. Nowak, R.M. May, *Virus Dynamics* (Oxford Univ. Press, 2000).

156. I. Bozic, M. A. Nowak, Resisting resistance. *Annu. Rev. Cancer Biol.* **1**, 203–221 (2017).

157. M. Slatkin, Fixation probabilities and fixation times in a subdivided population. *Evolution* **35**, 477–488 (1981).

158. H. A. Orr, The rate of adaptation in asexuals. *Genetics* **155**, 961–968 (2000).

159. M. C. Whitlock, Fixation probability and time in subdivided populations. *Genetics* **164**, 767–779 (2003).

160. C. O. Wilke, The speed of adaptation in large asexual populations. *Genetics* **167**, 2045–2053 (2004).

161. M. M. Desai, D. S. Fisher, A. W. Murray, The speed of evolution and maintenance of variation in asexual populations. *Curr. Biol.* **17**, 385–394 (2007).

162. W. B. Whitman, D. C. Coleman, W. J. Wiebe, Prokaryotes: The unseen majority. *Proc. Nat. Acad. Sci. U.S.A.* **95**, 6578–6583 (1998).

163. G. P. Wagner, V. J. Lynch, Evolutionary novelties. *Curr. Biol.* **20**, R48–R52 (2010).

164. A. Wagner, The molecular origins of evolutionary innovations. *Trends Genet.* **27**, 397–410 (2011).

165. A. C. Love, Evolutionary morphology, innovation, and the synthesis of evolutionary and developmental biology. *Biol. Philos.* **18**, 309–345 (2003).

166. J. Plucain, T. Hindré, M. Le Gac, O. Tenaillon, S. Cruveiller, C. Médigue, N. Leiby, W. R. Harcombe, C. J. Marx, R. E. Lenski, D. Schneider, Epistasis and allele specificity in the emergence of a stable polymorphism in *Escherichia coli*. *Science* **343**, 1366–1369 (2014).

167. K. Chatterjee, A. Pavlogiannis, B. Adlam, M. A. Nowak, The time scale of evolutionary trajectories. *PLOS Comput. Biol.* **10**, e1003818 (2014).

168. A. A. Pavlov, J. F. Kasting, Mass-independent fractionation of sulfur isotopes in Archean sediments: Strong evidence for an anoxic Archean atmosphere. *Astrobiology* **2**, 27–41 (2002).

169. C. A. Partin, A. Bekker, N. J. Planavsky, C. T. Scott, B. C. Gill, C. Li, V. Podkovyrov, A. Maslov, K. O. Konhauser, S. V. Lalonde, G. D. Love, S. W. Poulton, T. W. Lyons, Large-scale fluctuations in Precambrian atmospheric and oceanic oxygen levels from the record of U in shales. *Earth Planet. Sci. Lett.* **369–370**, 284–293 (2013).

170. A. Bachan, L. R. Kump, The rise of oxygen and siderite oxidation during the Lomagundi Event. *Proc. Nat. Acad. Sci. U.S.A.* **112**, 6562–6567 (2015).

171. L. R. Kump, A. E. Fallick, V. A. Melezhik, H. Strauss, A. Lepland, 8.1. The great oxidation event, in *Reading the Archive of Earth's Oxygenation, Volume 3: Global Events and the Fennoscandian Arctic Russia—Drilling Early Earth Project*, V. A. Melezhik A. R. Prave, E. J. Hanski, A. E. Fallick, A. Lepland, L. R. Kump, H. Strauss, Eds. (Springer-Verlag, 2013), pp. 1517– 1533.

172. D. C. Catling, K. J. Zahnle, C. P. McKay, Biogenic methane, hydrogen escape, and the irreversible oxidation of early Earth. *Science* **293**, 839–843 (2001).

173. N. Dijkstra, C. P. Slomp, T. Behrends, Vivianite is a key sink for phosphorus in sediments of the Landsort Deep, an intermittently anoxic deep basin in the Baltic Sea. *Chem. Geol.* **438**, 58–72 (2016).

174. L. A. Derry, Causes and consequences of mid-Proterozoic anoxia. *Geophys. Res. Lett.* **42**, 8538–8546 (2015).

175. T. A. Laakso, D. P. Schrag, Regulation of atmospheric oxygen during the Proterozoic. *Earth Planet. Sci. Lett.* **388**, 81–91 (2014).

176. C. Jones, S. Nomosatryo, S. A. Crowe, C. J. Bjerrum, D. E. Canfield, Iron oxides, divalent cations, silica, and the early earth phosphorus crisis. *Geology* **43**, 135–138 (2015).

177. C. T. Reinhard, N. J. Planavsky, B. C. Gill, K. Ozaki, L. J. Robbins, T. W. Lyons, W. W. Fischer, C. Wang, D. B. Cole, K. O. Konhauser, Evolution of the global phosphorus cycle. *Nature* **541**, 386–389 (2017).

178. J. F. Kasting, J. C. G. Walker, Limits on oxygen concentration in the prebiological atmosphere and the rate of abiotic fixation of nitrogen. *J. Geophys. Res.* **86**, 1147–1158 (1981).

179. A. Guskov, J. Kern, A. Gabdulkhakov, M. Broser, A. Zouni, W. Saenger, Cyanobacterial photosystem II at 2.9-Å resolution and the role of quinones, lipids, channels and chloride. *Nat. Struct. Mol. Biol.* **16**, 334–342 (2009).

180. L. M. Ward, J. Kirschvink, W. W. Fischer, Timescales of oxygenation following the evolution of oxygenic photosynthesis. *Orig. Life Evol. Biosph.* **46**, 51–65 (2016).

181. D. A. Gold, A. M. Caron, G. Fournier, R. E. Summons, Paleoproterozoic sterol biosynthesis and the rise of oxygen. *Nature* **543**, 420–423 (2017).

182. N. J. F. Blamey, U. Brand, J. Parnell, N. Spear, C. Lécuyer, K. Benison, F. Meng, P. Ni, Paradigm shift in determining Neoproterozoic atmospheric oxygen. *Geology* **44**, 651–654 (2016).

183. F. Horton, Did phosphorus derived from the weathering of large igneous provinces fertilize the Neoproterozoic ocean? *Geochem. Geophys. Geosyst.* **16**, 1723–1738 (2015).

184. G. M. Cox, G. P. Halverson, R. S. Stevenson, M. Vokaty, A. Poirier, M. Kunzmann, Z.-X. Li, S. Denyszyn, J. V. Strauss, F. A. Macdonald, A continental flood basalt weathering trigger for snowball Earth. *Earth Planet. Sci. Lett.* **446**, 89–99 (2016).

185. A. H. Knoll, M. J. Follows, A bottom-up perspective on ecosystem change in Mesozoic oceans. *Proc. Biol. Sci.* **283**, 20161755 (2016).

186. E. S. Vrba, Environment and evolution: Alternative causes of the temporal distribution of evolutionary events. *S. Afr. J. Sci.* **81**, 229–236 (1985).

187. W. Bains, D. Schulze-Makuch, Mechanisms of evolutionary innovation point to genetic control logic as the key difference between prokaryotes and eukaryotes. *J. Mol. Evol.* **81**, 34–53 (2015).

188. D. H. Erwin, Novelty and innovation in the history of life. *Curr. Biol.* **25**, R930–R940 (2015).

189. P. R. Crane, E. M. Friis, K. R. Pedersen, The origin and early diversification of angiosperms. *Nature* **374**, 27–33 (1995).

190. C. Darwin, *On the Origin of Species by Means of Natural Selection* (J. Murray, 1859).

191. C. Lyell, *Principles of Geology* (J. Murray, 1830–1833).

192. J. D. Burchfield, Darwin and the dilemma of geological time. *Isis* **65**, 300–321 (1974).

Citation: A. H. Knoll, M. A. Nowak, The timetable of evolution. *Sci. Adv.* **3**, e1603076 (2017).

Science Advances

The timetable of evolution

Andrew H. Knoll and Martin A. Nowak

ARTICLE TOOLS	http://advances.sciencemag.org/content/3/5/e1603076
REFERENCES	This article cites 176 articles, 74 of which you can access for free http://advances.sciencemag.org/content/3/5/e1603076#BIBL
PERMISSIONS	http://www.sciencemag.org/help/reprints-and-permissions